Orientation of a solid particle embedded in a monodomain nematic liquid crystal

Sergei V. Burylov
Transmag Research Institute, Ukrainian Academy of Sciences, Dnepropetrovsk, 320005, Ukraine

Yuri L. Raikher*
Departamento de Física, Universidade de Brasília, DF 70910 900, Brazil
(Received 14 October 1993; revised manuscript received 22 February 1994)

A problem of the equilibrium orientation of an elongated solid particle put inside a uniformly aligned nematic liquid crystal is studied. The particle is assumed to be sufficiently large so that the orientational distortions it causes may be treated in the framework of the continuum theory. Three kinds of anchoring of nematic material on the particle surface are considered: two of the planar, and one of the homeotropic type. We prove that, depending on the anchoring strength, the stable orientation of the particle major axis may be either perpendicular (weak anchoring) or parallel (strong anchoring) to the unperturbed director of the liquid-crystalline domain. The dimensionless parameter controlling the situation is the ratio ω of the transverse size of the particle to the extrapolation length of the nematic material. The transition from the perpendicular to the parallel orientation of the particle takes place at $\omega \sim 1$.

PACS number(s): 61.30.Gd, 75.50.Mm, 82.70.Kj, 61.30.Jf

INTRODUCTION

The subject of our consideration is the orientation of a solid elongated particle that is put inside a uniformly aligned nematic liquid crystal. The solution of this problem is essential to understand properties and behavior of any liquid-crystalline suspension. As examples of the latter we would like to refer to (i) ferroliquid crystals—the suspensions of single-domain ferroparticles in ordinary liquid crystals [1–4] and (ii) liquid-crystalline polymer melts or solutions either intentionally filled up with some reinforcing particles or "self-filled" with a certain amount of the still persisting true crystallites of the same material [5]. Yet more fascinating systems are solid magnetic [6] or nonmagnetic [7] particles of colloidal size inherently present in biological liquid-crystalline tissues like cellular membranes.

As to the ferroliquid crystals, they are relatively new composite materials which, unlike ordinary liquid crystals (LC), are very sensitive to the applied magnetic field. The chances of creation and the would-be unique properties of such suspensions were first explored by Brochard and de Gennes [1]. Later on, on the basis of concepts and estimations given in [1], primarily lyotropic nematic and cholesteric [2,8], then thermotropic nematic [3] and lyotropic smectic [4] systems had been prepared and were being studied.

In general, these experiments had confirmed the existence of considerable orientational and concentrational effects in ferroliquid crystals, but had raised a lot of questions as well.

On the list of problems one has to clarify, number one stands the problem of the type and strength of the orientational coupling between a particle and its aligned molecular environment. In other words, the question is, if a particle were put amidst a liquid crystal domain and set free, what will be its equilibrium orientation or (for an assembly) the equilibrium orientational distribution of particles? Until now the answer has been known only for two limiting cases, namely, of strong [1] and weak [9] anchoring. Herein we present the extended solution of the problem valid for an arbitrary anchoring strength.

The plan of the paper is as follows. In Sec. I we list the types of the orientational boundary conditions on the particle surface which would be taken for trial, and write down a general expression for the free energy of a system *particle plus liquid crystal.* The latter is done in a two-constant approximation as referred to the Frank moduli. In Secs. II and III, which are mostly calculational ones and thus may be skipped at the first reading, we derive the director distributions and energy increments caused by a cylindrical particle with its axis $\boldsymbol{\nu}$ either parallel or perpendicular to the unperturbed director $\boldsymbol{n}_0$ of a monodomain nematic LC. In Sec. IV we discuss the structure of nonsingular disclinations raised by a particle whose axis is perpendicular to $\boldsymbol{n}_0$, and propose a simple formula for the core radius of such a distortion entity valid for arbitrary finite anchoring strength. In Sec. V by comparing the energies $\mathcal{F}_{\parallel}$ and $\mathcal{F}_{\perp}$, where the subscripts indicate the relative directions of $\boldsymbol{\nu}$ and $\boldsymbol{n}_0$, we show that depending upon the values of pertinent material parameters of LC and the particle radius, the equilibrium state of the particle may be either $\boldsymbol{\nu} \parallel \boldsymbol{n}_0$ or $\boldsymbol{\nu} \perp \boldsymbol{n}_0$, and we give the necessary estimates.

I. THE FREE-ENERGY EXPRESSION. LONGITUDINAL ANCHORING

Let us formulate the problem we are dealing with in more detail. We consider an elongated solid particle (say, a rodlike one) with the length L and the transverse size $D \ll L$. Both L and D are much greater

*Permanent address: Institute of Continuous Media Mechanics, Urals Branch of The Russian Academy of Sciences, Perm, 614061, Russia.

than the dimensions of the molecules of the liquid crystal, and so relative to it the particle is a macroscopic object. (For example, in the thermotropic ferronematic [3,10] the particles with $L \simeq 3.5 \times 10^{-5}$ cm and $L/D \simeq 7$ were used.) The said particle is put inside a bulk of a uniformly aligned nematic liquid crystal whose orientation is fixed far from the particle site by the boundary conditions on the container walls, for example. The "tension" of the molecular alignment is proportional to the orientational-elastic (Frank) moduli K_{1-3} [11]. In principle, all three Frank moduli are different. However, to simplify our results, we shall use a "semi-isotropic" approximation setting $K_1 = K_3$, thus reducing the number of independent elastic coefficients to two. Equality $K_1 = K_3$ holds reasonably well for usual nematic liquid crystals, such as MBBA.

The surface of the particle is able to orient or "anchor" the adjacent liquid crystal molecules in one way or another. The degree of that anchoring is characterized by the surface energy density W, that is, the anisotropic part of the surface tension for a given pair of the solid substance and liquid crystal. To describe it, we shall use a simple model expression, first proposed by Rapini, written (see [11]) as

$$W(\gamma, \delta) = \tfrac{1}{2}\left(W_\theta \sin^2\gamma + W_\phi \sin^2\delta\right) . \qquad (1)$$

To define the angles γ and δ, at any point of the particle surface one introduces a local coordinate system with the polar axis along the normal to the particle. In this system the easy-orientation direction is determined by two angles, namely, the meridional α lying in the plane normal to the particle, and the azimuthal one, β, lying in the tangential plane. Any deviation of actual director orientation (α', β') from the direction (α, β) demanded by the surface energy is denoted by

$$\gamma = \alpha - \alpha' , \qquad \delta = \beta - \beta' .$$

Assuming, as usual, that the energy increment is diagonal in angular displacements, one arrives at expression (1), where W_θ and W_ϕ are the characteristic energies of the out-of-plane (meridional) and in-plane (azimuthal) director perturbations, respectively. The reference plane here is the local tangent one. As is well known, both W's may be, and often are, easily modified by special treatment of the solid surfaces [12].

In what follows we evaluate the free energy of the system comprising the particle and the liquid crystal surrounding it, and by minimization find the equilibrium, i.e., the lowest-energy orientational state of the particle for several types of anchoring conditions. The present problem is closely connected with the classical one, where, assuming some particular anchoring on solid unmovable walls enclosing liquid crystal, one determines the orientational distribution of the latter. Only now the framework is reversed inside out, and we have to find the orientation of the particle (movable solid walls) whereas the alignment of the nematic at infinity stays put.

Pursuing the scheme adopted in Ref. [1], we split the possible anchoring conditions into three "mutually orthogonal" configurations, viz., *longitudinal*—the easy (i.e., energetically favored) direction on the particle surface is parallel to the main axis $\boldsymbol{\nu}$ of the particle; *circular*—the easy direction is perpendicular to the main axis $\boldsymbol{\nu}$, and is tangential to the particle surface; *homeotropic*—the easy direction is normal to the particle surface.

To obtain the desired expression for the free energy of the system, one should sum up both the volume and surface contributions of the orientational-elastic origin produced by the particle's presence, and integrate them over the LC specimen volume and the particle surface, respectively. In the "semi-isotropic" two-constant approximation for the Frank moduli and with the Rapini formula (1) for the surface term, one gets

$$\mathcal{F} = \tfrac{1}{2}\left\{\int_V \Big[K_1(\mathrm{div}\boldsymbol{n})^2 + K_2(\boldsymbol{n}\cdot\mathrm{curl}\boldsymbol{n})^2 + K_1(\boldsymbol{n}\times\mathrm{curl}\boldsymbol{n})^2\Big]\, dV + \int_S \left[W_\theta \sin^2\gamma + W_\phi \sin^2\delta\right] dS\right\}, \qquad (2)$$

where $\boldsymbol{n}(\boldsymbol{r})$ is the nematic director and γ and δ are the angle deviations of the latter from the easy-orientation directions on the surface. Below, making use of the condition $D/L \ll 1$ (elongated particle), we shall neglect the director distortions induced by the end walls of the particle.

Now let us consider sequentially the above-listed cases of anchoring. It is apparent that in the longitudinal situation our model does not provide any real choice: the particle will always set its main axis $\boldsymbol{\nu}$ along the unperturbed director $\boldsymbol{n}_0$ unless the temperature is so high that the aligning influence of the LC matrix becomes comparable with $k_B T$ (for quantitative estimation see below).

II. CIRCULAR ANCHORING

For the circular anchoring, as it follows from the symmetry considerations, two orientations can compete to be the lowest-energy ones: $\boldsymbol{\nu} \perp \boldsymbol{n}_0$ and $\boldsymbol{\nu} \parallel \boldsymbol{n}_0$. (We remind the reader that vector $\boldsymbol{\nu}$ is the unit vector of the particle main axis, and $\boldsymbol{n}_0$ is the unperturbed director of the nematic domain.) So, it is sufficient to evaluate the corresponding values $\mathcal{F}_\perp$ and $\mathcal{F}_\parallel$ of formula (2), and compare them. To be particular, from now on we assume that the particle has the form of a circular cylinder, and denote its transverse size as $D = 2R$, with R being the cylinder radius.

A. Perpendicular case ($\boldsymbol{\nu} \perp \boldsymbol{n}_0$)

The director distribution around the particle is sketched in Fig. 1(a). In the notations given there the orientational field may be written as

$$\boldsymbol{n} = (\cos\Phi,\ \sin\Phi,\ 0) , \qquad \Phi = \Phi(r, \varphi) , \qquad (3)$$

which transforms the free energy (2) into

$$\mathcal{F}_\perp = \tfrac{1}{2}\left[K_1 \int (\nabla\Phi)^2\, dV + W_\theta \int \sin^2(\Phi_{0S} - \Phi_S)\, dS\right] , \qquad (4)$$

where Φ_{0S} is the angle of the easy orientation on the particle surface and $\Phi_S = \Phi(R, \varphi)$. Note that for the director distribution (3) vectors $\boldsymbol{n}$ and curl$\boldsymbol{n}$ are always orthogonal, and thus the term in Eq. (2) which is proportional to K_2 (twist) is an identical zero.

For Φ_{0S} under the circular anchoring conditions one should set

$$\Phi_{0S} = \begin{cases} \varphi - \frac{1}{2}\pi & \text{for } 0 < \varphi < \pi \\ \varphi - \frac{3}{2}\pi & \text{for } \pi < \varphi < 2\pi \end{cases} . \qquad (5)$$

Minimization of the functional (4) with respect to Φ and Φ_S yields

$$\nabla^2\Phi = 0\,, \qquad 2K_1 \left.\frac{\partial\Phi}{\partial r}\right|_R = W_\theta \sin\left[2(\Phi_S - \Phi_{0S})\right]\,, \quad (6)$$

i.e., the two-dimensional Laplace equation accompanied by the specific boundary condition. We choose the general form of solution as

$$\Phi(r, \varphi) = \sum_{n=0}^{\infty} (R/r)^n \left(u_n \sin n\varphi + v_n \cos n\varphi\right). \qquad (7)$$

Substituting it into the boundary condition given by Eqs. (6), the set of equations for the Fourier coefficients u_n and v_n is obtained:

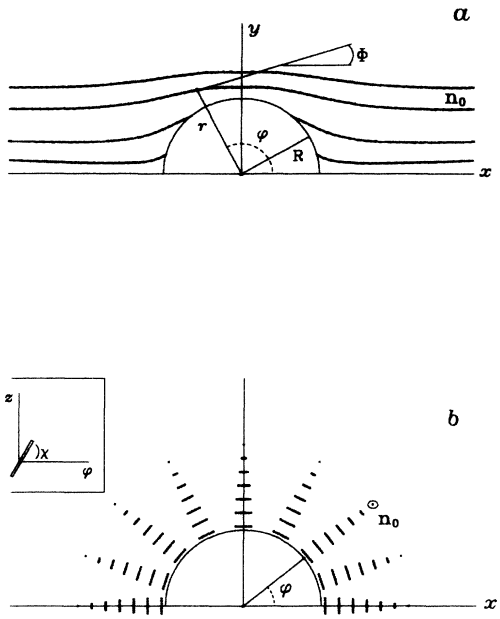

FIG. 1. Schematic representation of the director distribution around a cylindrical particle with circular anchoring for $\boldsymbol{\nu} \perp \boldsymbol{n}_0$ (a) and $\boldsymbol{\nu} \parallel \boldsymbol{n}_0$ (b).

$$\sum_{n=0}^{\infty} n(u_n \sin n\varphi + v_n \cos n\varphi) - \tfrac{1}{2}\omega_\theta \sin\left(2\Phi_{0S} - 2\sum_{n=0}^{\infty}(u_n \sin n\varphi + v_n \cos n\varphi)\right) = 0\,. \qquad (8)$$

Here we have introduced the dimensionless ratio

$$\omega_\theta = W_\theta R/K_1\,, \qquad (9)$$

which relates the surface and volume energy contributions. Apparently, ω_θ is the only material parameter affecting the character of the sought for solutions.

The symmetry conditions easily understandable from Fig. 1(a) read

$$\Phi(r, -\varphi) = -\Phi(r, \varphi)\,, \quad \Phi(r, \pi - \varphi) = -\Phi(r, \varphi)\,. \quad (10)$$

Application of Eqs. (10) to the expansion (7) gives

$$\Phi(r, \varphi) = \sum_{m=1}^{\infty} (R/r)^{2m} u_{2m} \sin(2m\varphi)\,, \qquad (11)$$

thus reducing the number of the nonzero coefficients to that of u_n with the even index. Then Eq. (8) transforms into

$$2\sum_{m=1}^{\infty} m\, u_{2m} \sin(2m\varphi) - \tfrac{1}{2}\omega_\theta \sin\left(2\Phi_{0S} - 2\sum_{m=1}^{\infty} u_{2m} \sin(2m\varphi)\right) = 0\,. \quad (12)$$

Multiplying it by $\sin 2k\varphi$ and integrating over the azimuth angle, we arrive at the infinite set of equations

$$k\, u_{2k} - \frac{\omega_\theta}{4\pi}\int_0^{2\pi} \sin\left(2\Phi_{0S} - 2\sum_{m=1}^{\infty} u_{2m} \sin(2m\varphi)\right) \times \sin(2k\varphi)\, d\varphi = 0\,, \quad (13)$$

for the amplitudes $u_{2k}(\omega_\theta)$.

Let us choose the solution of Eq. (13) in the form

$$u_{2k} = -p^k(\omega_\theta)/k\,, \qquad (14)$$

thus introducing a non-negative function $p(\omega_\theta)$. Though the exact expression for $p(\omega_\theta)$ is yet unknown, we can point out its limiting values

$$p = \begin{cases} 0 & \text{for } \omega_\theta = 0 \\ 1 & \text{for } \omega_\theta = \infty\,. \end{cases} \qquad (15)$$

The first line of this relation is obvious, since zero anchoring induces no distortions. The second line is explained by the equalities

$$\Phi_{0S} = \Phi_S(\omega_\theta = \infty) = -\sum_{k=1}^{\infty} k^{-1} \sin(2k\varphi)\,, \qquad (16)$$

where the last one is proven in Ref. [1].

For the adopted choice of u_{2k} the expansion (11) readily sums up, yielding

$$\Phi_S = -\arctan\left(\frac{p\sin 2\varphi}{1-p\cos 2\varphi}\right), \qquad \Phi_{0S} = -\arctan\left(\frac{\sin 2\varphi}{1-\cos 2\varphi}\right), \tag{17}$$

where we have made use of relation (16) as well. Substitution of the surface angles (18) into Eq. (13) gives

$$-p^k + \frac{\omega_\theta}{4\pi}\int_0^{2\pi} \sin\left\{2\left[\arctan\left(\frac{\sin 2\varphi}{1-\cos 2\varphi}\right) - \arctan\left(\frac{p\sin 2\varphi}{1-p\cos 2\varphi}\right)\right]\right\} \sin(2k\varphi)\, d\varphi = 0, \tag{18}$$

which after somewhat tedious but simple transformations takes the form

$$p^k = \frac{1}{4\pi}\,\omega_\theta(1-p^2)\int_0^{2\pi} \frac{\sin 2\varphi \sin(2k\varphi)}{1-2p\cos 2\varphi + p^2}\, d\varphi. \tag{19}$$

The integral in the right-hand side is a known one, and equals πp^{k-1}. Therefore Eq. (19) finally reduces to

$$p^2 + (4/\omega_\theta)p - 1 = 0,$$

whose only positive root is

$$p = (2/\omega_\theta)\left[\sqrt{1+\tfrac{1}{4}\omega_\theta^2} - 1\right]. \tag{20}$$

Let us check up on this expression for the already known limiting cases. At weak anchoring we get

$$p(\omega_\theta) = \omega_\theta/4 \qquad (\omega_\theta \ll 1),$$

in accordance with the result found in [9], and at strong anchoring Eq. (20) yields

$$p(\omega_\theta) = 1 - 2/\omega_\theta + 2/\omega_\theta^2 \qquad (\omega_\theta \gg 1),$$

which leads to $p(\infty) = 1$ given in Ref. [1]. The complete solution (11) with allowance for Eq. (14) takes the form

$$\Phi(r,\varphi) = -\arctan\left[\frac{(R/r)^2 p\sin 2\varphi}{1-(R/r)^2 p\cos 2\varphi}\right], \tag{21}$$

where $p(\omega_\theta)$ is rendered by Eq. (20).

The last step in obtaining the energy $\mathcal{F}_\perp$ is to evaluate expression (1) for $\Phi(r,\varphi)$ from Eq. (21). Integrating the first term in Eq. (4) by parts, and thus reducing all the integrations to those over the particle surface, we get

$$\mathcal{F}_\perp/L = -\tfrac{1}{2}R\int_0^{2\pi}[K_1\,\Phi_S\nabla_r\Phi|_S - W_\theta\sin^2(\Phi_{0S}-\Phi_S)]d\varphi. \tag{22}$$

Here we have taken into account that at infinity $\Phi(r,\varphi) = 0$, and complied to the rule that the surface integral ought to change sign when the outward normal is replaced by the inward one. For convenience, in Eq. (22) we use the linear density of the free energy per unit length of the particle long axis.

From Eq. (21) it follows that

$$\nabla_r\,\Phi|_S = \frac{2}{R}\,\frac{p\sin 2\varphi}{1-2p\cos 2\varphi + p^2}, \tag{23}$$

and thus the volume contribution to $\mathcal{F}_\perp$ is

$$\mathcal{F}_\perp^{(v)}/L = K_1\sum_{k=1}^{\infty}\frac{1}{k}p^{k+1}\int_0^{2\pi}\frac{\sin 2\varphi\sin(2k\varphi)}{1-2p\cos 2\varphi+p^2}\,d\varphi.$$

Since the last integral coincides with that of Eq. (19), the result comes out immediately,

$$\mathcal{F}_\perp^{(v)}/L = \pi K_1\sum_{k=1}^{\infty}\frac{1}{k}\,p^{2k} = -\pi K_1\ln(1-p^2). \tag{24}$$

For the second term of Eq. (22), using the usual trigonometric identities and formulas (18), we get

$$\mathcal{F}_\perp^{(s)}/L = \tfrac{1}{2}W_\theta R(1-p)^2\int_0^{2\pi}\frac{\cos^2\varphi}{1-2p\cos 2\varphi+p^2}\,d\varphi = \tfrac{1}{2}\pi W_\theta R(1-p). \tag{25}$$

From Eqs. (24) and (25) for the net free energy induced in a uniform nematic by a particle with the circular boundary condition in orientation $\boldsymbol{\nu}\perp\boldsymbol{n}_0$ it follows that

$$\mathcal{F}_\perp = \pi K_1 L\left[-\ln(1-p^2) + \tfrac{1}{2}\omega_\theta(1-p)\right]. \tag{26}$$

To decide whether this configuration is indeed favored in the LC, we should compare it to the similar quantity $\mathcal{F}_\parallel$ evaluated for the parallel case.

B. Parallel case ($\boldsymbol{\nu}\parallel\boldsymbol{n}_0$)

The corresponding director distribution is shown in Fig. 1(b). There we use the cylindrical set of coordinates with the polar axis along $\boldsymbol{\nu}$ and $\boldsymbol{n}_0$, whence

$$\boldsymbol{n} = (0,\ \cos\chi,\ \sin\chi). \tag{27}$$

The angle $\chi(r)$—see insertion in Fig. 1(b)—describes the director orientation in the φ-z plane of the local framework. The easy orientation direction on the particle surface is $\chi_{0S} = 0$. The conditions imposed on χ at infinity are

$$\left.\frac{d\chi}{dr}\right|_\infty = 0, \qquad \chi(\infty) = \tfrac{1}{2}\pi. \tag{28}$$

Its value $\chi_S = \chi(R)$ is yet to be found.

Due to the independence of χ on the azimuth angle, the general expression (2) after substitution of the director representation (27) readily integrates over φ and z, yielding

$$\mathcal{F}_{\parallel} = \pi(1+\varepsilon)^{-1} K_1 L \left[\int_{\ln R}^{\infty} \left(\chi'^2 - \chi' \sin 2\chi + \cos^2\chi + \varepsilon \cos^4\chi \right) d\xi + \omega_\phi (1+\varepsilon) \sin^2 \chi_S \right], \tag{29}$$

where $\xi = \ln r$ and $\chi' = d\chi/d\xi$. Here we have introduced the parameter

$$\varepsilon = (K_1 - K_2)/K_2 = (K_3 - K_2)/K_2 \tag{30}$$

(in our approach $K_1 = K_3$) and, similar to Eq. (9),

$$\omega_\phi = W_\phi R/K_1 . \tag{31}$$

Variation of the functional (29) with respect to χ and χ_S gives the set of equations

$$\chi'' + \left(\tfrac{1}{2} + \varepsilon \cos^2\chi\right) \sin 2\chi = 0 ,$$
$$\chi' \Big|_R - \tfrac{1}{2} \left[1 + (1+\varepsilon)\omega_\phi\right] \sin 2\chi_S = 0 , \tag{32}$$

which together with conditions (28) forms a closed boundary problem. A simplified form of the latter had already been addressed in Ref. [9]. Similar calculations applied to Eq. (32) yield a closed albeit implicit solution

$$\frac{\sqrt{1+\varepsilon\cos^2\chi} + \sin\chi}{\sqrt{1+\varepsilon\cos^2\chi} - \sin\chi} \frac{\sqrt{1+\varepsilon\cos^2\chi_S} - \sin\chi_S}{\sqrt{1+\varepsilon\cos^2\chi_S} + \sin\chi_S} = \left(\frac{r}{R}\right)^2 , \tag{33}$$

where χ_S is evaluated from the equation

$$\cos\chi_S \left\{ \sqrt{1+\varepsilon\cos^2\chi_S} - \left[1 + (1+\varepsilon)\omega_\phi\right] \sin\chi_S \right\} = 0 . \tag{34}$$

One of its roots is trivial: $\chi_S^{(1)} = \frac{1}{2}\pi$, and with the use of Eq. (33) reduces the energy functional (29) to

$$\mathcal{F}_{\parallel}^{(1)} = \pi K_1 L \omega_\phi . \tag{35}$$

The second root cannot be found explicitly. The corresponding procedure of evaluating the free energy is presented in the Appendix. Its result—see formula (A11)—reads

$$\mathcal{F}_{\parallel}^{(2)} = \pi K_1 L \frac{1}{\sqrt{\varepsilon}} \arctan\left(\frac{\omega_\phi \sqrt{\varepsilon}}{1+\omega_\phi}\right) . \tag{36}$$

To choose between the values found for $\mathcal{F}_{\parallel}$, let us consider their ratio. It may be written as

$$\mathcal{F}_{\parallel}^{(2)}/\mathcal{F}_{\parallel}^{(1)} = (1+\omega_\phi)^{-1} \arctan(x)/x ,$$
$$x = \omega_\phi \sqrt{\varepsilon}/(1+\omega_\phi) .$$

Since, according to our definitions (30) and (31), the parameters ε and ω_ϕ are positive, it is easy to see that the considered ratio is always less than unity, reaching it only at $\omega_\phi \to \infty$. That means that the sought minimal value of $\mathcal{F}_{\parallel}$ is the one provided by expression (36).

III. HOMEOTROPIC ANCHORING

Here we evaluate the energies of the alternative orientations of a particle when the anchoring condition favors the normal molecular alignment on its surface. Due to that, from the very beginning we are able to set $W_\phi = 0$ in formula (2). Pursuing the lines of the preceding section, first we address the perpendicular case.

A. Perpendicular case ($\nu \perp n_0$)

The director distribution around the particle is schematically shown in Fig. 2(a). Choosing the angle variable $\Phi(r, \varphi)$ so that it complies with the parametrization (3), we have to replace expressions (5) by

$$\Phi_{0S} = \begin{cases} \varphi & \text{for } -\frac{1}{2}\pi < \varphi < \frac{1}{2}\pi \\ \varphi - \pi & \text{for } \frac{1}{2}\pi < \varphi < \frac{3}{2}\pi . \end{cases} \tag{37}$$

The only manifestation of this change is that from now on the integrals should be taken over the interval $[-\frac{1}{2}\pi, \frac{3}{2}\pi]$. Save for that, formulas (3)–(13) remain intact. For the Fourier coefficients u_{2k} we now set

$$u_{2k} = (-1)^{k+1} p^k/k , \tag{38}$$

that yields

$$\Phi_S = \arctan\left(\frac{p \sin 2\varphi}{1 + p\cos 2\varphi}\right) ,$$
$$\Phi_{0S} = \arctan\left(\frac{\sin 2\varphi}{1 + \cos 2\varphi}\right) , \tag{39}$$

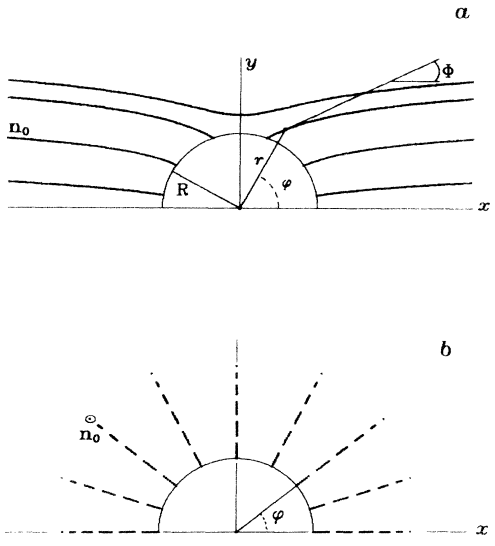

FIG. 2. Schematic representation of the director distribution around a cylindrical particle with homeotropic anchoring for $\nu \perp n_0$ (a) and $\nu \parallel n_0$ (b).

cf. Eq. (17). Substitution of Eqs. (38) and (39) into (13) gives the equation

$$(-p)^k + \frac{\omega_\theta}{4\pi}\int_0^{2\pi} \sin\left\{2\left[\arctan\left(\frac{\sin 2\varphi}{1+\cos 2\varphi}\right) - \arctan\left(\frac{p\sin 2\varphi}{1+p\cos 2\varphi}\right)\right]\right\} \sin(2k\varphi)\, d\varphi = 0\,, \quad (40)$$

which after similar transformations as for Eq. (18), delivers exactly the same result as Eq. (20) for the function $p(\omega_\theta)$. Using it, one finds

$$\Phi(r,\varphi) = \arctan\left[\frac{(R/r)^2 p \sin 2\varphi}{1+(R/r)^2 p\cos 2\varphi}\right]\,, \quad (41)$$

cf. Eq. (21). With the aid of formula (22) and

$$\nabla_r \Phi|_S = -\frac{2}{R}\,\frac{p\sin 2\varphi}{1+2p\cos 2\varphi+p^2}\,,$$

we get for the perpendicular orientation energy of the particle with homeotropic anchoring

$$\mathcal{F}_\perp = \pi K_1 L\left[-\ln(1-p^2) + \tfrac{1}{2}\omega_\theta(1-p)\right]\,.$$

The result turns out to be the same as for the circular surface alignment— see the preceding section. This exact coincidence would not look so surprising if one recalls that all the terms in the distortion energy expression are sensitive only to relative deviations of the director. Because of that, in energy calculations the actual absolute orientation of the easy axis on the surface is to a certain extent irrelevant as far as the anchoring strength W_θ remains constant.

B. Parallel case ($\nu \parallel n_0$)

The corresponding sketch is shown in Fig. 2(b). In the cylindrical coordinate system one has

$$\boldsymbol{n} = (\cos\chi,\ 0,\ \sin\chi)\,,$$

where again $\chi(r)$ is the deviation of $\boldsymbol{n}(\boldsymbol{r})$ from the easy alignment direction $\chi_{0S} = 0$. For this two-dimensional nonuniformity, as for Eq. (3), the free-energy expression does not contain terms proportional to K_2. Thus in the approximation adopted ($K_1 = K_3 \neq K_2$), it reads

$$\mathcal{F}_\parallel = \pi K_1 L\left[\int_{\ln R}^{\infty}\left(\chi'^2 - \chi'\sin 2\chi\cos^2\chi\right)\, d\xi + \omega_\phi \sin^2\chi_S\right]\,. \quad (42)$$

Functional (42) coincides with that already analyzed in Ref. [9]. Its minimum value, obtained there, is

$$\mathcal{F}_\parallel = \pi K_1 L\omega_\theta/(1+\omega_\theta)\,. \quad (43)$$

IV. DIRECTOR TEXTURES AROUND A CYLINDRICAL PARTICLE

Let us consider in more detail the orientational textures around a cylindrical particle whose axis is perpendicular to the nonperturbed director of the nematic domain. The general views of the corresponding patterns are shown in Figs. 1(a) and 2(a). We remark that the isolines of orientation in those figures were plotted numerically by integration of the equation $dy/dx = \tan\Phi$ at $\omega_\theta = 0.5$ with Φ taken from formulas (21) and (41), respectively.

The elastic energies of these configurations are given by one and the same expression,

$$\mathcal{F}_\perp = \pi K_1 L\left[-\ln(1-p^2) + \tfrac{1}{2}\omega_\theta(1-p)\right]\,, \quad (44)$$

$$p = (2/\omega_\theta)\left[\sqrt{1+\tfrac{1}{4}\omega_\theta^2} - 1\right]\,, \qquad \omega_\theta = W_\theta R/K_1\,,$$

where the anchoring strength W_θ is arbitrary.

The presence of the logarithmic term in the expression for $\mathcal{F}_\perp$ and the topography of the director field around the azimuths $\varphi = 0,\ \pi$ in Fig. 1(a) and $\varphi = \pi/2,\ 3\pi/2$ in Fig. 2(a) point out that in fact we are dealing with nonsingular plane disclinations. The latter are produced by finite objects (closed surfaces) put inside a uniform orientation field. Their role is to provide continuous adjustment of the director directions in the vicinity of an alien object and at infinity. From expansion of Eq. (44) at $\omega \to \infty$ one finds that in this limit the distortion energy reduces to a customary disclination logarithm

$$\mathcal{F}_\perp \approx \pi K_1 L \ln\left(\frac{R}{b}\right)\,, \quad (45)$$

where $b = K_1/W_\theta$ is the extrapolation length.

Let us compare our result with that given in Ref. [1],

$$\mathcal{F}_\perp = \pi K_1 L \ln\left(\frac{R}{a}\right)\,, \quad (46)$$

obtained in the rigid (infinitely strong, $W_\theta = \infty$) anchoring approximation. There a is a cutoff distance with the meaning of the radius of the disclination core which is usually set equal to the molecular size of the liquid crystal.

The similarity of formulas (45) and (46) is apparent. It is more important to emphasize their essential difference. While Eq. (45) is the result of a consistent application of the continuum theory, Eq. (46) is introduced to the latter from outside, and is based on general physical reasons. It reminds us that the continuum theory may not be applied at distances less than a. Therefore Eq. (46) must replace (45) when the extrapolation length becomes smaller than the molecular size.

Inside the validity range of Eqs. (44), (45), i.e., at $b > a$, which is rather wide, our results yield a simple way to make explicit evaluation of the director patterns and energies of nonsingular disclinations. Conventionally, those disclinations are described (see Ref. [13], for

example) by a phenomenological energy linear density function

$$\mathcal{F}_{\text{eff}}/L = \pi K \ln(R/r_c),$$

where R is the reference curvature radius of the closed surface, and r_c is the radius of the disclination "core" depending upon W and K. Setting

$$\mathcal{F}_\perp = \mathcal{F}_{\text{eff}},$$

where $\mathcal{F}_\perp$ is taken from Eqs. (44), and omitting the surface terms, we get the explicit expression for the core size of a nonsingular disclination

$$r_c = \left(8R/\omega_\theta^2\right)\left(\sqrt{1+\omega_\theta^2/4}-1\right), \qquad (47)$$

with limiting behavior

$$r_c = \begin{cases} R & \text{for } R \ll K_1/W_\theta \quad \text{(weak anchoring)} \\ 4K_1/W_\theta & \text{for } R \gg K_1/W_\theta \quad \text{(strong anchoring).} \end{cases}$$

Thus we see that the effective radius is the monotonically decreasing function of $\omega_\theta = W_\theta R/K_1$ going down from the real geometrical size R of the curved boundary to the value $4b$ which is of the order of magnitude of the extrapolation length, and is no longer sensitive to the size of the object that causes the orientational defect.

Therefore the above-presented formulas deliver a detailed description of the director field around the particle for all the range of anchoring strengths compatible with the macroscopic theory of elasticity of LC. In particular, if W could be increased separately due to, for example, temperature (the existence of such an effect has been reported in [14] for several thermotropic nematics including the most famous one—MBBA), formulas (21) and (41) are capable of demonstrating how the smooth continuous director distortions tighten gradually, tending to transform themselves into well-pronounced orientational defects.

To illustrate this tendency, in Fig. 3 we show the schematic patterns of the molecular orientation in the layer adjacent to the particle surface. There also are presented the angular distributions calculated according to formulas (37) and (41), of director on the particle surface for the homeotropic case with $\boldsymbol{\nu} \perp \boldsymbol{n}_0$. Three considerably different values of the parameter ω_θ are taken to display the evolution of the orientation field upon the change of the anchoring strength.

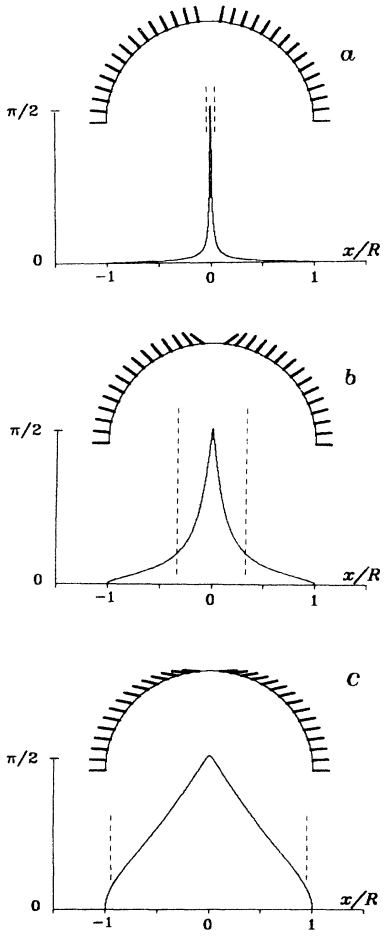

FIG. 3. Patterns of molecular orientation on the particle surface (semicircles), and the surface angular deviations $|\Phi - \Phi_{0S}|$ at different cross sections of the cylinder by planes x/R =const. The relative orientation of $\boldsymbol{\nu}$ and $\boldsymbol{n}_0$ is that of Fig. 2(a). The dimensionless anchoring parameter ω_θ is 100 (a), 10 (b), and 1 (c). Dashed vertical lines show the effective diameter $2r_c$ of the nonsingular disclination determined by formula (47).

V. EQUILIBRIUM ORIENTATIONS OF A CYLINDRICAL PARTICLE

Having in disposition the expressions for the energy increments $\mathcal{F}_\perp$ and $\mathcal{F}_\parallel$, it is easy to compare them and determine the equilibrium orientation of a particle relative to $\boldsymbol{n}_0$.

For circular anchoring, according to Sec. II, one has

$$\mathcal{F}_\perp/\pi K_1 L = -\ln(1-p^2) + \tfrac{1}{2}\omega_\theta(1-p),$$
$$\mathcal{F}_\parallel/\pi K_1 L = \frac{1}{\sqrt{\varepsilon}} \arctan\left(\frac{\omega_\phi\sqrt{\varepsilon}}{1+\omega_\phi}\right), \qquad (48)$$

where $p = p(\omega_\theta)$—see Eq. (20). These formulas contain three independent material parameters, viz., ω_θ, ω_ϕ, and ε. Due to that the direct comparison of Eqs. (48), though easy for any particular system, is too cumbersome to be done in general. To get a qualitative impression, we set $\omega_\theta = \omega_\phi = \omega$, which, according to Ref. [12], is often approximately so, and take either $\varepsilon = 0$ (single-constant approximation with regard to the Frank moduli) or $\varepsilon = 1$ which is valid by the order of magnitude for nematics like MBBA.

The results of comparison are shown in Fig. 4. The intersections of the curves yield that equation $\mathcal{F}_\perp = \mathcal{F}_\parallel(\varepsilon = 0)$ has the root $\omega_1 = 1.396$, and $\mathcal{F}_\perp = \mathcal{F}_\parallel(\varepsilon = 1)$ has the

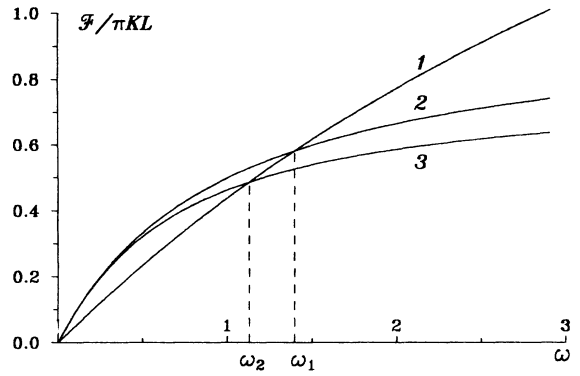

FIG. 4. Orientational energies as functions of the dimensionless parameter $\omega = WR/K$ according to formulas (48) and (49). Curve 1—$\mathcal{F}_\perp$, curve 2—$\mathcal{F}_\parallel(\varepsilon = 0)$, curve 3—$\mathcal{F}_\parallel(\varepsilon = 1)$.

root $\omega_2 = 1.128$. Note that the parameter ε (the difference between K_1 and K_2), even if changed considerably, only weakly affects the actual value of the root.

In each case the root ω_i divides the whole range of ω in two domains. For $\omega < \omega_i$ one has $\mathcal{F}_\perp < \mathcal{F}_\parallel$, and thus the equilibrium orientation of the particle is that with $\boldsymbol{\nu} \perp \boldsymbol{n}_0$, whereas for $\omega > \omega_i$ the condition $\mathcal{F}_\perp > \mathcal{F}_\parallel$ prescribes $\boldsymbol{\nu} \parallel \boldsymbol{n}_0$. At $\omega = \omega_i$ the orientation of the particle is completely degenerated against the unperturbed director. In fact, due to the orientational Brownian motion, the angular degeneracy of the particle axis should take place not only at $\omega = \omega_i$ but within a certain interval $2\Delta\omega$ around this point. The value of $\Delta\omega$ is defined by condition

$$\Delta\omega \gg k_B T / \tfrac{\partial}{\partial\omega} \left| \mathcal{F}_\perp - \mathcal{F}_\parallel \right|_{\omega=\omega_i} .$$

To make the estimate quantitative, let us assume that "much greater" means the difference by one order of magnitude. Then with the aid of formulas (48) we get

$$\Delta\omega \approx 2\, k_B T / KL.$$

For a thermotropic nematic with a reference value $K \approx 5 \times 10^{-7}$ dyn at room temperature it yields $\Delta\omega \approx 1.5 \times 10^{-7}/L$. Setting $L \approx 3.5 \times 10^{-5}$ cm, as it was in [3,10], we get $\Delta\omega \approx 5 \times 10^{-3}$, which proves that normally the interval of the indeterminacy of the particle orientation is not large.

For homeotropic anchoring the set of expressions to be compared is derived in Sec. III. It reads

$$\begin{aligned} \mathcal{F}_\perp / \pi K_1 L &= -\ln(1-p^2) + \tfrac{1}{2}\omega_\theta\,(1-p)\,, \\ \mathcal{F}_\parallel / \pi K_1 L &= \omega_\theta/(1+\omega_\theta)\,, \end{aligned} \tag{49}$$

and contains only one combination of the material parameters—ω_θ. Therefore in this case the comparison may be done in general. Figure 4 displays it as well. One has only to assume that its abscissa is ω_θ, and not pay attention to curve 3. The characteristic value of ω_θ separating the regions of parallel and perpendicular equilibrium orientations is then $\omega_\theta = \omega_1 = 1.396$.

Consideration of the energies of the orthogonal states ($\boldsymbol{\nu} \perp \boldsymbol{n}_0$) and ($\boldsymbol{\nu} \parallel \boldsymbol{n}_0$), which are certain extrema of the functional (2), immediately raises the question about the general form of $\mathcal{F}(\vartheta)$, where ϑ denotes the angle between $\boldsymbol{\nu}$ and $\boldsymbol{n}_0$. Unfortunately, its analytical derivation seems hardly possible due to the loss of symmetry of the director distribution at arbitrary ϑ. So, one has to restrict oneself by qualitative considerations. First, it is apparent that the proper argument should be $\cos^2\vartheta = (\boldsymbol{\nu}\cdot\boldsymbol{n}_0)^2$, since in our problem all the physically meaningful quantities ought to be bilinear in both unit vectors. Secondly, though we do not consider the three-dimensional perturbations $\delta\boldsymbol{n}$, it looks natural to assume that the smaller of the values of $\mathcal{F}_\perp$ and $\mathcal{F}_\parallel$ at given ω corresponds to the true minimum of $\mathcal{F}(\cos^2\vartheta)$. The question of whether the greater one is the maximum still has no explicit answer. However, we surmise that it is really so. This had been proven in [1] for $\omega \to \infty$, and in Ref. [9] for $\omega \ll 1$. In the latter paper we had shown that the angular dependence of $\mathcal{F}$ is as simple as

$$\mathcal{F}(\cos^2\vartheta) = \mathcal{F}_\perp + \left(\mathcal{F}_\parallel - \mathcal{F}_\perp\right)\cos^2\vartheta\,.$$

Because of a very limited set of material parameters entering the model, it seems highly improbable that at $\omega \sim 1$ there might appear some contribution delivering extra maxima of $\mathcal{F}(\cos^2\vartheta)$. On this basis we conclude that at any given ω (except maybe close vicinities of the points 0 and ω_i) there exists one and only one stable orientational state of the particle. It means, in turn, that in an assembly of such particles (with circular or homeotropic anchoring) with the growth of ω an orientational transition of the "easy-plane" – "easy-axis" kind should take place.

As it has been stated in the introductory remarks, the particular objects of our interest are liquid-crystalline suspensions. That means that real particles which we intend to apply our results to are rather small, 10^{-2}–$10\,\mu$m in linear size. Now let us check up for what range of particle dimensions the peculiarities of the orientational states found out at $\omega \sim 1$ are relevant.

According to the literature (see [12,15], for example) the range of possible values of W is several decades wide, spreading from 10^{-4} to 1 erg/cm^2 depending on the nature, quality, and treatment of the solid surfaces. The values of the Frank moduli are not so uncertain and stand $K \sim 5 \times 10^{-7}$ erg/cm for thermotropic and an order of magnitude less for lyotropic nematics. These data place the extrapolation length $b = K/W$ in the range $5 \times 10^{-8} - 5 \times 10^{-3}$ cm, which is probably too wide since having been determined via the extremities. Omitting a decade at each end, we see that the values $\omega \sim 1$ correspond to $R \sim 5 \times 10^{-7} - 5 \times 10^{-4}$ cm, i.e., $50 - 5 \times 10^4$ Å, which is exactly the reference range of the particle size used in colloids and suspensions.

The above-presented theory in its initial version [9], i.e., for $\omega \ll 1$, had already proved to be helpful [16–18] in both qualitative and quantitative explanation of the orientational-optical effects induced by external magnetic field in thermotropic ferronematics. The particular case

we have dealt with in Refs. [16–18] was the homeotropic anchoring.

CONCLUSION

Embedding of an anisometric (elongated) solid particle in a nematic liquid crystal causes the effective orientational coupling between the particle axis and the director field of the nematic. This coupling comes from the anisotropy of anchoring of the nematic molecules on the particle surface. For particles of a characteristic size starting from that pertinent to colloids and suspensions, the effective coupling energy may be derived in the framework of the macroscopic (continuum) theory, and, under some physically justified assumptions, expressed as a set of rather simple relations.

The formulas obtained show that depending upon the type and strength of anchoring, the equilibrium position of a particle may be either parallel or perpendicular to the director of a liquid crystal domain. The principal parameter governing the situation is the ratio of the particle radius to the extrapolation length of the nematic.

According to all the evidence existing the considered coupling is the main mechanism determining the basic (in the absence of external fields) orientational state of liquid-crystalline suspensions.

The effects discussed, since they are predicted in the framework of a macroscopic theory, should not be so difficult to observe (as it had been first remarked in Ref. [1]) in large-scale experiments, e.g., if we study with a polarizing microscope a behavior of a zero-buoyancy rod with appropriately treated surface floating in a nematic slab of a sufficient thickness.

APPENDIX: EVALUATION OF THE ENERGY FUNCTIONAL FOR THE NONTRIVIAL ROOT OF EQ. (34)

According to Eq. (34), its sought for root $\chi_S^{(2)}$ is to be found from the relation

$$1+(1+\varepsilon)\omega_\phi = \sqrt{1+\varepsilon\cos^2\chi_S^{(2)}}/\sin\chi_S^{(2)} . \qquad \text{(A1)}$$

Substitution into Eq. (33) yields

$$\frac{\sqrt{1+\varepsilon\cos^2\chi}+\sin\chi}{\sqrt{1+\varepsilon\cos^2\chi}-\sin\chi}\,\frac{(1+\varepsilon)\omega_\phi}{2+(1+\varepsilon)\omega_\phi} = \left(\frac{r}{R}\right)^2 . \qquad \text{(A2)}$$

Introducing a notation

$$q = \sqrt{1+\varepsilon\cos^2\chi}/\sin\chi , \qquad \text{(A3)}$$

one may rewrite Eq. (A2) as

$$\frac{q+1}{q-1}\,\frac{(1+\varepsilon)\omega_\phi}{2+(1+\varepsilon)\omega_\phi} = \left(\frac{r}{R}\right)^2 , \qquad \text{(A4)}$$

whence

$$q = \frac{[2+(1+\varepsilon)\omega_\phi]r^2+(1+\varepsilon)\omega_\phi R^2}{[2+(1+\varepsilon)\omega_\phi]r^2-(1+\varepsilon)\omega_\phi R^2} . \qquad \text{(A5)}$$

From definition (A3), we have

$$\sin\chi = \sqrt{\frac{1+\varepsilon}{\varepsilon+q^2}} , \qquad \cos\chi = \sqrt{\frac{q^2-1}{\varepsilon+q^2}} . \qquad \text{(A6)}$$

Now it is easy to evaluate the surface contribution to the free energy (29):

$$\mathcal{F}^{(s)} = \pi K_1 L\omega_\phi \sin^2\chi_S^{(2)} = \pi K_1 L\omega_\phi \frac{1+\varepsilon}{\varepsilon+q^2}\bigg|_S .$$

According to Eqs. (A1) and (A3),

$$q\Big|_S = 1+(1+\varepsilon)\omega_\phi ,$$

and hence

$$\mathcal{F}^{(s)} = \pi K_1 L\frac{(1+\varepsilon)\omega_\phi}{\varepsilon+[1+(1+\varepsilon)\omega_\phi]^2} . \qquad \text{(A7)}$$

To deal with the volume contribution of Eq. (29), let us rewrite it in terms of the parameter q. Taking into account that from Eq. (33)

$$\chi' = \cos(\chi)\sqrt{1+\varepsilon\cos^2\chi} ,$$

one finds

$$\mathcal{F}^{(v)} = 2\pi K_1 L(1+\varepsilon)^{-1}\int_{\ln R}^{\infty} d\xi\,\sqrt{1+\varepsilon\cos^2\chi} \times\left[\sqrt{1+\varepsilon\cos^2\chi}-\sin\chi\right]\cos^2\chi ,$$

and with the aid of Eqs. (A6)

$$\mathcal{F}^{(v)} = 2\pi K_1 L\int_R^\infty \frac{dr}{r}\,\frac{q(q+1)(q-1)^2}{(\varepsilon+q^2)^2} . \qquad \text{(A8)}$$

From Eq. (A4) it follows that

$$dr/r = dq/(1-q^2) ,$$

so that Eq. (A8) transforms into

$$\mathcal{F}^{(v)} = 2\pi K_1 L\int_1^{1+(1+\varepsilon)\,\omega_\phi} dq\,\frac{q(q-1)}{(\varepsilon+q^2)^2} . \qquad \text{(A9)}$$

The last integral can be taken in terms of elementary functions, that yields

$$\mathcal{F}^{(v)} = \pi K_1 L\left\{\frac{1}{\sqrt{\varepsilon}}\arctan\left(\frac{\omega_\phi\sqrt{\varepsilon}}{1+\omega_\phi}\right) - \frac{(1+\varepsilon)\omega_\phi}{\varepsilon+\left[1+(1+\varepsilon)\omega_\phi\right]^2}\right\} . \qquad \text{(A10)}$$

Adding Eqs. (A7) and (A10), one eventually obtains

$$\mathcal{F}_{\|} = \mathcal{F}^{(s)} + \mathcal{F}^{(v)} = \pi K_1 L \frac{1}{\sqrt{\varepsilon}} \arctan\left(\frac{\omega_\phi \sqrt{\varepsilon}}{1+\omega_\phi}\right), \tag{A11}$$

i.e., formula (36).

Let us have a look at some limiting cases for energy expressions (A11). For $\varepsilon \ll 1$, using the power series for the arctan function, one gets

$$\mathcal{F}_{\|} = \pi K_1 L \sum_{k=0}^{\infty} \frac{(-1)^k}{(2k+1)\sqrt{\varepsilon}} \left(\frac{\omega_\phi \sqrt{\varepsilon}}{1+\omega_\phi}\right)^{2k+1} \approx \pi K_1 L \frac{\omega_\phi}{1+\omega_\phi}\left[1 - \tfrac{1}{3}\varepsilon\left(\frac{\omega_\phi}{1+\omega_\phi}\right)^2\right], \tag{A12}$$

which is valid for arbitrary ω_ϕ. In the single-constant approximation ($K_1 = K_2 = K_3$) formula (A12) recovers the corresponding result of Ref. [9]: $\mathcal{F}_{\|} = \pi K L \omega_\phi/(1+\omega_\phi)$.

At $\omega_\phi \to \infty$, i.e., in rigid anchoring approximation, from Eq. (A12) it follows that

$$\mathcal{F}_{\|} = \pi K_1 L(1 - \varepsilon/3 - 1/\omega_\phi) + \cdots,$$

which is valid for arbitrary ω_ϕ. In the single-constant approximation ($K_1 = K_2 = K_3$) formula (A12) recovers the corresponding result of Ref. [9]: $\mathcal{F}_{\|} = \pi K L \omega_\phi/(1+\omega_\phi)$.

$$\mathcal{F}_{\|} = \pi K_1 L \omega_\phi \left[1 - \omega_\phi + (1-\varepsilon/3)\,\omega_\phi^2\right] + \cdots.$$

[1] F. Brochard and P. G. de Gennes, J. Phys. **31**, 691 (1970).

[2] L. Liebert and A. Martinet, J. Phys. Lett. **40**, 363 (1979).

[3] S.-H. Chen and N. M. Amer, Phys. Rev. Lett. **51**, 2298 (1983).

[4] P. Fabre, C. Cassagrande, M. Veyssié, V. Cabuil, and R. Massart, Phys. Rev. Lett. **64**, 539 (1990).

[5] *Liquid Crystalline Order in Polymers*, edited by A. Blumstein (Academic Press, New York, 1978).

[6] *Magnetite Biomineralization and Magnetoreception in Organisms. A New Biomagnetism*, edited by J. L. Kirshvink, D. S. Jones, and B. J. MacFadden (Plenum Press, New York, 1985).

[7] G. H. Brown and J. J. Wolken, *Liquid Crystals and Biological Structures* (Academic Press, New York, 1979).

[8] A. M. Figueiredo Neto, L. Liebert, and A. M. Levelut, J. Phys. (Paris) **45**, 1505 (1984).

[9] S. V. Burylov and Yu. L. Raikher, Phys. Lett. A **149**, 279 (1990).

[10] B. J. Liang and S.-H. Chen, Phys. Rev. A **39**, 1441 (1989).

[11] P. G. de Gennes, *The Physics of Liquid Crystals* (Clarendon Press, Oxford, 1974).

[12] J. Cognard, *Alignment of Nematic Liquid Crystals and Their Mixtures* (Gordon and Breach, London, 1982).

[13] A. V. Kovalchuk, M. V. Kurik, O. D. Lavrentovich, and V. V. Sergan, Zh. Eksp. Teor. Fiz. **94**, 350 (1988) [Sov. Phys. JETP **67**, 1065 (1988)].

[14] J. S. Patel and H. Yokoyama, Nature (London) **362**, 525 (1993).

[15] L. M. Blinov, E. I. Katz, and A. A. Sonin, Usp. Fiz. Nauk. **152**, 449 (1987) [Sov. Phys. Usp. **30**, 604 (1987)].

[16] S. V. Burylov and Yu. L. Raikher, J. Magn. Magn. Mater. **85**, 74 (1990).

[17] S. V. Burylov and Yu. L. Raikher, Izv. Akad. Nauk. SSSR, Ser. Fiz. **55**, 1127 (1991) [Bull. Acad. Sci. USSR, Phys. Ser. **55**, 87 (1991)].

[18] S. V. Burylov and Yu. L. Raikher, J. Magn. Magn. Mater. **122**, 62 (1993).